

Evolution of metastable quasi-regular structures in heated wavy liquid films

V. Lel · H. Stadler · A. Pavlenko · R. Kneer

Received: 9 May 2005 / Accepted: 16 August 2006 / Published online: 18 October 2006
© Springer-Verlag 2006

Abstract Formation and development of quasi-regular, metastable structures within laminar wavy falling films were studied using IR-thermography. These structures emerge within the residual layer between large waves. It is shown that the typical size of regular structures does not depend on the liquid flow rate and is in the order of magnitude of the critical length of the Rayleigh–Taylor instability. Also a model of thermal-capillary breakdown on the basis of a simplified force balance between the surface tension and the tangential stress as well as the energy balance in the residual layer is presented. Model predictions and experimental data are in good agreement.

List of symbols

a_{IR}	coefficient of absorption of radiation energy (m^{-1})
a	temperature conductivity ($\text{m}^2 \text{s}^{-1}$)
c_p	specific heat ($\text{J kg}^{-1} \text{K}^{-1}$)
c_w	velocity of large waves (m s^{-1})
f_w	frequency of large waves (s^{-1})
g	gravitational force (m s^{-2})
Ka	Kapitza number $\frac{\sigma^3 \rho}{g \mu^4}$
l_x	length scale in x direction (m)
l_z	length scale in z direction (m)

L	length of heat section (m)
Ma_c	Marangoni number $\frac{q_w \left \frac{d\sigma}{dT} \right }{\lambda \rho U_s^2}$
Ma_q	Marangoni number $\frac{q_w \left \frac{d\sigma}{dT} \right \left(\frac{v^2}{g} \right)^{\frac{2}{3}}}{\lambda \rho v^2}$
NETD	noise equivalent temperature difference (K)
Pr	Prandtl number $Pr = \frac{\nu}{a}$
q_w	heat flux on the wall surface (W m^{-2})
Re	Reynolds number $Re = \frac{\Gamma}{\nu}$
t	time (s)
t_{TC}	time of thermal-capillary breakdown (s)
t_w	time between passing of two consecutive wave crest
T	temperature (K)
T_{in}	inflow temperature (K)
ΔT	difference between inflow and local surface temperature (K)
u	velocity (m s^{-1})
U_0	average velocity of the film (m s^{-1})
U_s	average velocity of the gas–liquid interface (m s^{-1})
U_{res}	average velocity of residual layer (m s^{-1})
U_{TC}	typical thermal-capillary velocity (m s^{-1})
x	stream wise coordinate (m)
y	coordinate perpendicular to flow (m)
z	coordinate (m)

Greek characters

δ_{res}	thickness of residual layer (m)
Γ	liquid flow rate per unit length ($\text{m}^2 \text{s}^{-1}$)
λ	thermal conductivity ($\text{W m}^{-1} \text{K}^{-1}$)
λ_w	wavelength of large waves (m)
Λ	transverse size of regular structures (m)
Λ_0	critical length of Rayleigh–Taylor instability $2\pi \sqrt{\frac{\sigma}{(\rho_l - \rho_g)g}}$ (m)

V. Lel (✉) · H. Stadler · R. Kneer
Institute of Heat and Mass Transfer,
RWTH Aachen University, Aachen, Germany
e-mail: lel@wsa.rwth-aachen.de

A. Pavlenko
Institute of Thermophysics, Siberian Branch,
Russian Academy of Sciences, Novosibirsk, Russia
e-mail: pavl@itp.nsc.ru

$\sqrt{3}\Lambda_0$	wavelength of maximum growth of Rayleigh–Taylor instability (m)
μ	dynamic viscosity ($\text{kg m}^{-1} \text{s}^{-1}$)
ν	kinematic viscosity ($\text{m}^2 \text{s}^{-1}$)
ρ	density (kg m^{-3})
ρ_{IR}	reflection degree
σ	Surface tension (N m^{-1})
$\frac{d\sigma}{dT}$	coefficient of temperature alteration of surface tension ($\text{N m}^{-1} \text{K}$)

1 Introduction

Liquid film flows are widely used in industrial apparatuses such as heat exchangers, condensers and evaporators. They are also applied in cryogenic equipment and for cooling in nuclear reactors. The usage of falling film flows can be explained by the high heat transfer coefficient coming along with a low pressure drop [12]. A decrease in the thickness of the film leads to an increase in the heat transfer coefficient. However, very thin films are prone to breakdowns, the appearance of dry spots and, as a consequence, to a drastic reduction of the heat transfer between the fluid and the surface which may lead to thermal destruction of a cooling element. There are several mechanisms leading to the appearance of dry spots: liquid evaporation within the residual layer, i.e. between large waves, film separation due to a gas flow, boiling crisis in the liquid film, thermal-diffusive and thermal-capillary breakdown of the film due to a gradient in the concentration of the components in the mixture or a temperature gradient on the surface of the film. In this paper only thermal-capillary mechanisms of dry spot appearance are considered.

Prediction of the critical heat flux is very important in the theory of heat transfer in film flow. Several models for thermal-capillary breakdown of falling films are published. For instance, in [7] it is stated that thermal-capillary breakdown of a laminar wavy liquid falling film only occurs in the residual layer between large waves. According to [7], a necessary condition for film breakdown is, that the time required for thermal-capillary breakdown of a film is less or equal than the time difference between two consecutive large waves. With a rise of the liquid flow rate the thickness of the residual layer becomes sufficiently high, so that the time required for breakdown formation is longer than the time between two consecutive wave crests. Ganchev [7] developed a 2D model of the breakdown, where the thermal-capillary forces transfer the fluid from the residual layer to a large wave in counter

current flow, whereas our analysis indicates that the problem is highly three-dimensional.

Using the π -theorem, Gimbutis [8] derives the dimensionless parameter Ma_q for the determination of the critical heat flux associated with the formation of dry spots. Experimental data from other authors for laminar-wavy and turbulent film flow of water along tubes with a height up to 2 m was generalised using Marangoni and Reynolds numbers.

In [9] the 2D model of dry spot appearance is presented, too. The model was derived on the basis of simplified equations of mass and momentum conservation. Areas of film surface instability were identified depending on the heat flux and on the wave length of large waves. Thereby a critical heat flux leading to thermal capillary breakdown could be determined.

A model in which the distinctive three-dimensional flow of the fluid within the residual layer is taken into consideration is presented in [3]. In this work the dependency on the heat flux was obtained on the basis of a simplified balance of forces, including thermal-capillary forces and the energy balance in the film. Furthermore, the assumption was made that the typical thermal-capillary velocity is several times higher than the typical liquid velocity in flow direction within the residual layer. A drawback of this model is that an assumption about the characteristic sizes alongside and across the flow is necessary. According to [3] these sizes are equal. The authors in [15] have generalised the model from [3] with regards to evaporation on the surface of the film. The final formula for the critical heat flux includes the dependency obtained in [3] as well as the terms for capillarity-induced interfacial evaporation and the streamwise thermal-capillary effect. The ratio of the characteristic streamwise temperature drop to the typical length in this direction was determined by generalising experimental data.

In [6], the critical heat flux at which thermal capillary breakdown occurs in a liquid film is expressed in terms of the equilibrium wetting angle. In contrast to this the experimental study of [16] shows that breakdown of the non-isothermal liquid film is defined by thermo-capillary forces and that the wetting angle has almost no effect.

Thermal-capillary phenomena in the range of low Reynolds numbers at slightly inclined heating surfaces were studied experimentally in [11]. For laminar flow without waves, regular structures in the form of thick jets as well as areas with a thin film or dry spots between the jets were found on the surface of the heater.

Qualitatively jet formation in laminar-wavy flow was visualised in [5] with a photographic camera. Both, the surface temperature, which is the driving potential for

thermo-capillary effects, and the film thickness, which results from the force-balance, have not been experimentally studied. Investigations [13, 14] also revealed the presence of regular structures in the form of alternating jets and dry spots in the flow of saturated laminar-wavy liquid film with intensive evaporation or boiling.

The aim of this work is the experimental investigation of the evolution of regular structures in the residual layer of subcooled laminar-wavy liquid films. Especially the quantitative influence of the heat flux and of external wave excitation on the surface temperature distribution and hence on the hydrodynamics of falling films were studied using IR-thermography. A model of thermal-capillary breakdown of the falling film has been derived.

2 Experimental setup

The closed-loop test facility is shown in Fig. 1. Silicone fluid is supplied from a liquid distributor through an adjustable gap onto the 150 mm wide test section. The test section consists of a vertical polyvinylchloride plate with a copper plate ($130 \times 70 \text{ mm}^2$) mounted in the hydrodynamically established region 330 mm downstream of the distribution gap. At the end of the test section the liquid film flows into a reservoir. The

fluid is circulated by an adjustable piston pump. The flow rate is measured by a positive displacement flow meter. The experiments were carried out in a Reynolds number range between 2 and 39. The variation of Reynolds numbers was limited by the pump capacity. The entrance temperature of the liquid T_1 is checked by a thermocouple in the liquid distributor and is kept constant using a heat exchanger in the lower reservoir. Also, for safety reasons the liquid temperature T_2 is monitored with a thermocouple at a vertical position parallel to the measurement area. In order to avoid disturbances of the film flow this thermocouple is displaced sideways. The temperatures T_4 within the heater is measured at eight measurement points at distances of 6 and 10 mm from the surface. To excite regular waves on the liquid surface a loudspeaker above the upper reservoir is used.

The heat flux is regulated by adjusting the voltage supplied to heating cartridges in the copper plate. The average heat flux in the experiments was set between 0 and $3.1 \times 10^4 \text{ W m}^{-2}$. An error less than 3% was assessed taking into account that heat losses through the isolation can be neglected. Silicone oils (Polydimethylsiloxane [DMS-T]) of different viscosity were used as test fluids to allow for a variation of the Prandtl number Pr between 57 and 167. The material properties of the different liquids are presented in Table 1. Experiments have been carried out at atmospheric

Fig. 1 Scheme of experimental setup

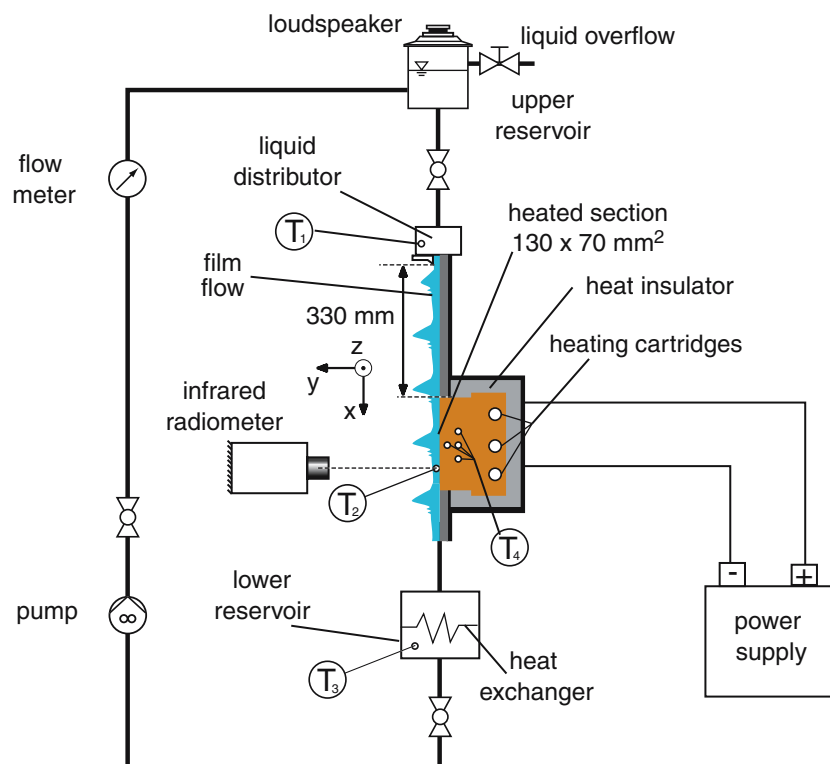


Table 1 Physical properties for silicone fluids
Polydimethylsiloxane (DMS-T) at $T = 25^\circ\text{C}$

	DMS-T05	DMS-T11	DMS-T12
ρ (kg m^{-3})	918	938	950
ν ($\text{m}^2 \text{s}^{-1}$) (10^{-6})	4.78	8.5	16.5
dv/dT ($\text{m}^2 \text{K}^{-1} \text{s}^{-1}$) (10^{-8})	-7.37	-13.88	-26.04
σ (N m^{-1})	0.0197	0.0201	0.0206
$d\sigma/dT$ ($\text{N K}^{-1} \text{m}^{-1}$) (10^{-5})	-6.7	-6.7	-6.7
c_p ($\text{J kg}^{-1} \text{K}^{-1}$)	1,546	1,546	1,546
λ ($\text{W m}^{-1} \text{K}^{-1}$)	0.119	0.136	0.145
ρ_{IR} ($9.0 \mu\text{m} < \lambda < 9.5 \mu\text{m}$) (-)	0.049	0.052	0.055
$Pr = \nu/a$ (-)	57	91	167
$Ka = (\sigma^3 \rho)/(g \mu^4)$ (-)	1,931,670	192,344	14,037

pressure and ambient temperature. For the time-resolved recording of the temperature field an IR-camera CEDIP JADE 3 LW with a 320×240 HgCdTe focal-plane-array has been used. The camera operates in the long wavelength region between 7.7 and 9.5 μm . Using an additional filter which transmits radiation only above a wavelength of 9.0 μm it is possible to measure the temperature in a very thin layer of the surface of the film [1]. According to measurements conducted at the Institute for Organic Chemistry at RWTH Aachen university the average absorption coefficient of the fluids at wavelengths between 9.0 and 9.5 μm is between $a_{\text{IR}} = 3 \times 10^5$ and $a_{\text{IR}} = 4 \times 10^5 \text{ m}^{-1}$. Average reflection coefficients in the relevant range of wavelengths are included in Table 1.

The sensitivity (NETD) of this camera is about 25 mK. The integration time of the IR-camera varies depending on the range of working temperatures. For the given range of temperatures it was set to 500 μs . For a given set of parameters the film flow was recorded over a period of 5 s at a frame rate of 200 Hz. The surface area recorded was $70 \times 108 \text{ mm}$. This is equivalent to a resolution of $0.33 \times 0.33 \text{ mm}^2$ per pixel.

3 Regular structures within the residual layer

The surface temperature records of the falling liquid film are shown in Figs. 2 and 3. In Fig. 2 results from the film flow with natural waves are shown, whereas Fig. 3 refers to excited film flow. In these figures individual pictures were scaled to show the minimum temperature (inflow temperature) in black and the maximum temperature in red. ΔT is the difference between inflow and local surface temperature.

In Fig. 2 the frames recorded at a heat flux of $0.4 \times 10^4 \text{ W m}^{-2}$ are presented for three different silicone fluids with different Prandtl numbers. It is obvious that for high Prandtl numbers regular structures are not formed distinctly, Fig. 2a (DMS-T12, $Pr = 173$,

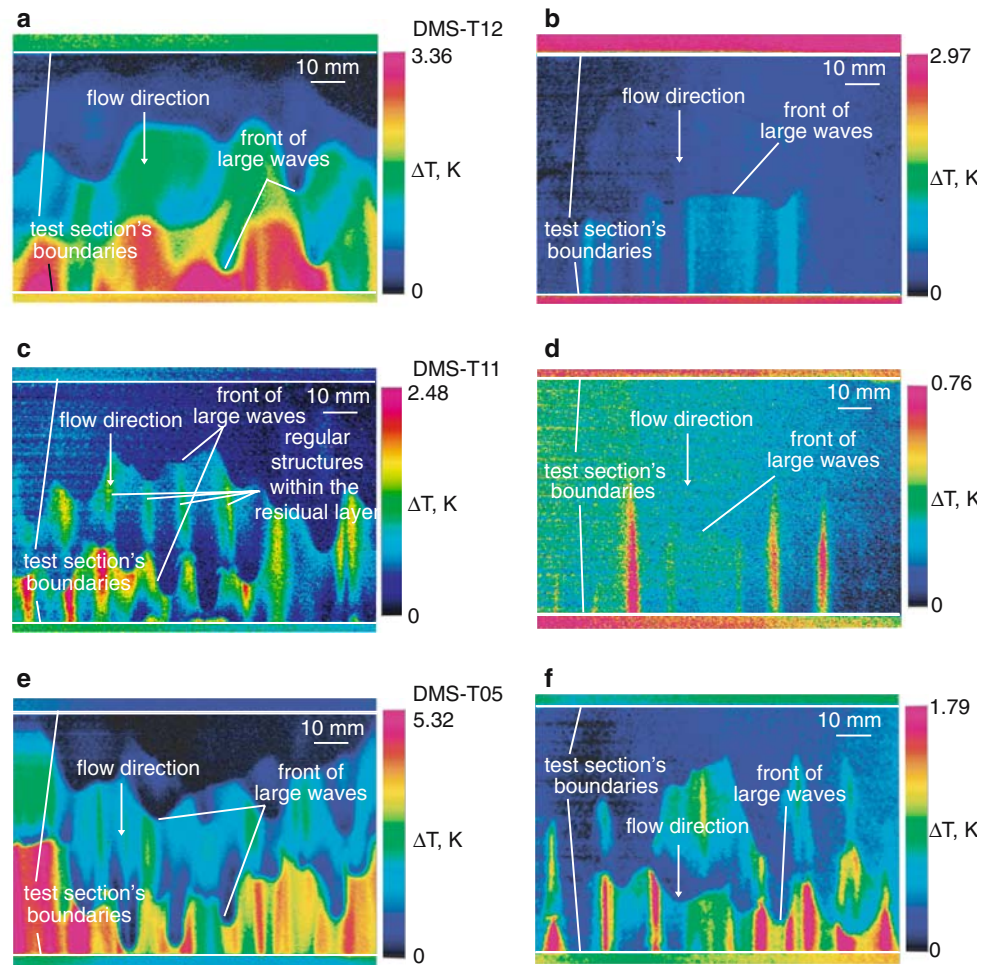
$Re = 2.3$) and Fig. 2b (DMS-T12, $Pr = 177$, $Re = 9.7$). This may be due to the fact that for this liquid viscous forces are significantly higher than thermal-capillary forces and also remain dominant despite the decrease in viscosity due to the rise in temperature.

For the liquid DMS-T11 with a lower viscosity ($Pr = 96$), distinct regular structures in the form of horizontally alternating areas (perpendicular to the flow direction) with increased and decreased temperatures can be seen within the residual layer between large waves, Fig. 2c. These regular structures reflect the intersection of large 3D waves on the surface. The front of 2D waves splits up into 3D drop-like formations/streaks carrying a major portion of the liquid. The zones with a very thin film between the drop-shaped waves within the residual layer are the origin for regular structures. In the regions of film thinning the liquid is heated significantly and temperature gradients develop on the surface causing thermal-capillary forces.

If the heat flux is kept constant, an increase in the liquid flow rate leads to less distinct structures (compare Fig. 2c and d with $Pr = 96$ and $Re = 10.0$ and $Re = 29.0$). This happens because the temperature difference at the surface of the film is reduced with increasing Reynolds number and, as a consequence, the influence of thermal-capillary forces decreases.

With a further reduction of the Prandtl number regular structures are still present; however, a decrease in the viscosity leads to a randomisation of the wave fronts in laminar-wavy film flow. This can be seen in Fig. 2e (DMS-T05, $Pr = 59$, $Re = 8.1$). From this picture it is clear that large waves become more oblong and concentrate in the area of low temperatures. Also, a considerable change in the flow structure of large waves takes place over length scales of the order of one wavelength. At $Pr = 60$ and $Re = 29.6$ the change in the form of large waves is not so obvious. Due to a thicker film the surface temperature gradients decrease as it was mentioned above and the influence on the flow structure is reduced.

Fig. 2 Thermographic pictures of the surface of undisturbed laminar-wavy liquid film, $q_w = 0.4 \times 10^4 \text{ W/m}^2$. **a** DMS-T12, $T_{in} = 22.7^\circ\text{C}$, $Pr = 173$, $Re = 2.3$; **b** DMS-T12, $T_{in} = 21.3^\circ\text{C}$, $Pr = 177$, $Re = 9.7$; **c** DMS-T11, $T_{in} = 21.1^\circ\text{C}$, $Pr = 96$, $Re = 10.0$; **d** DMS-T11, $T_{in} = 21.0^\circ\text{C}$, $Pr = 96$, $Re = 29.0$; **e** DMS-T05, $T_{in} = 22.3^\circ\text{C}$, $Pr = 59$, $Re = 8.1$; **f** DMS-T05, $T_{in} = 21.2^\circ\text{C}$, $Pr = 60$, $Re = 29.6$



In natural flow of laminar-wavy film a relatively wide bandwidth of wave lengths (frequencies) between consecutive wave fronts occurs. To study a more regular flow of a liquid film and to reduce the oscillation range, a loud speaker was used for excitation of a constant frequency. As it can be seen in Fig. 3a (DMS-T12, $Pr = 174$, $Re = 2.3$) regular structures are not fully developed. As described above this is caused by a high liquid viscosity and low temperature gradients on the surface.

An increase of the heat flux to a certain value leads to the formation of regular structures and dry spots, Fig. 3b (DMS-T12, $Pr = 164$, $Re = 2.7$, $q_w = 3.0 \times 10^4 \text{ W m}^{-2}$). In Fig. 3b it can also be seen that dry spots are located at a distance from each other corresponding to the typical length of regular structures. This emphasises that under the given conditions dry spot formation has a thermal-capillary nature.

In Fig. 3c (DMS-T11, $Pr = 96$, $Re = 12.2$) and Fig. 3d (DMS-T11, $Pr = 96$, $Re = 22.2$) the critical wavelength of the Rayleigh–Taylor instability $\Lambda_0 = 2\pi \sqrt{\frac{\sigma}{(\rho_l - \rho_g)g}}$ and the wavelength of maximum

growth of Rayleigh–Taylor instability $\sqrt{3}\Lambda_0$ are presented. According to the figure, these values are of the same order as the typical distance between regular structures within the residual layer.

In order to apply the Rayleigh–Taylor theory to the current problem, a coordinate system moving relative with the propagation velocity of the front of 2D waves has to be considered. In this coordinate system the initial situation of the classical Rayleigh–Taylor instability can be found. The liquid which is accumulated in the large waves has a high density and ‘rests’ above the gas which has a lower density. Perturbations with a wavelength longer than the critical wavelength of the Rayleigh–Taylor theory grow in time and can eventually be regarded as three dimensional. As it was mentioned before, the area with a lower liquid flow rate is formed at the boundary between two 3D waves. The lower film thickness leads to a better heating of the film in this area. Therefore the temperature gradient within the residual layer between hot and cold areas increases which is the driving potential for thermal-capillary flows of liquid.

Fig. 3 Thermographic pictures of the surface of excited laminar-wavy liquid film, $q_w = 0.6 \times 10^4 \text{ W/m}^2$ (except **b** $3.0 \times 10^4 \text{ W/m}^2$ and **c** $1.2 \times 10^4 \text{ W/m}^2$). **a** DMS-T12, $T_{in} = 22.5^\circ\text{C}$, $Pr = 174$, $Re = 2.3$; **b** DMS-T12, $T_{in} = 26.1^\circ\text{C}$, $Pr = 164$, $Re = 2.7$; **c** DMS-T11, $T_{in} = 21.0^\circ\text{C}$, $Pr = 96$, $Re = 12.2$; **d** DMS-T11, $T_{in} = 21.0^\circ\text{C}$, $Pr = 96$, $Re = 22.2$; **e** DMS-T05, $T_{in} = 21.8^\circ\text{C}$, $Pr = 60$, $Re = 11.0$; **f** DMS-T05, $T_{in} = 21.4^\circ\text{C}$, $Pr = 60$, $Re = 19.9$

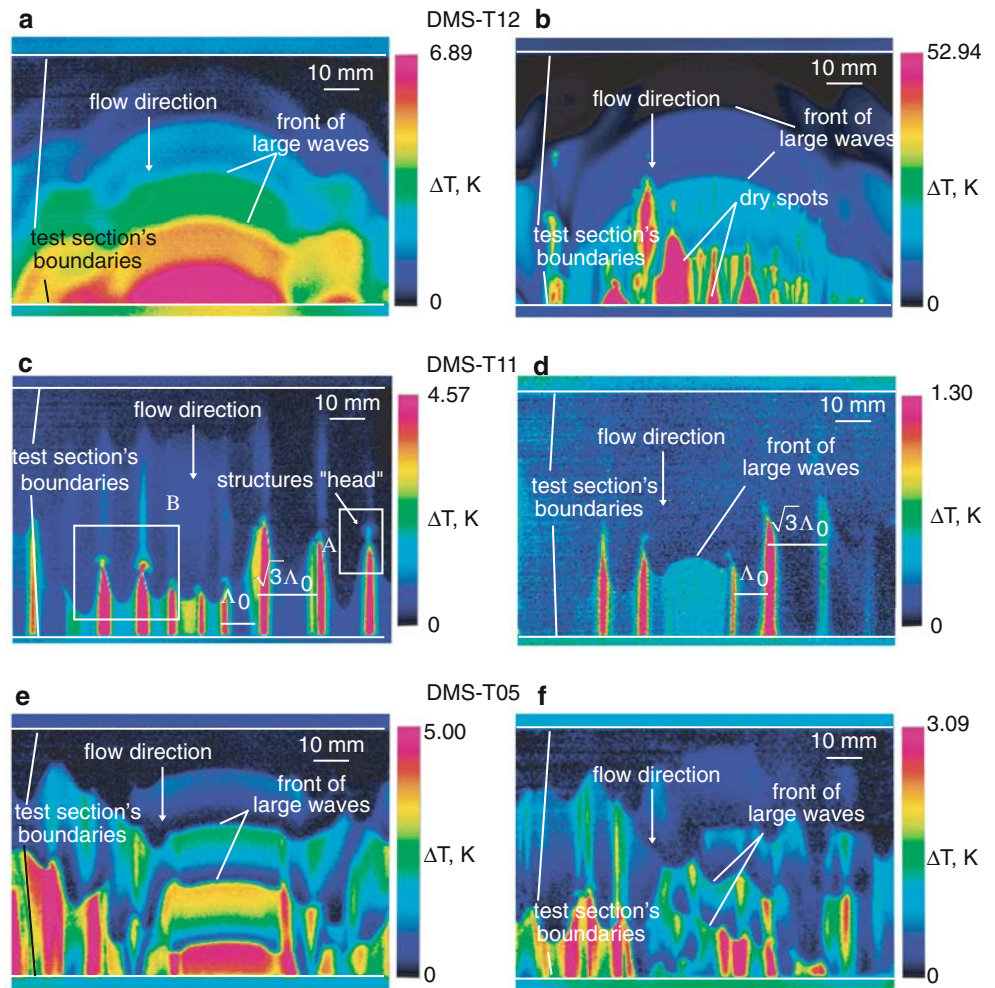
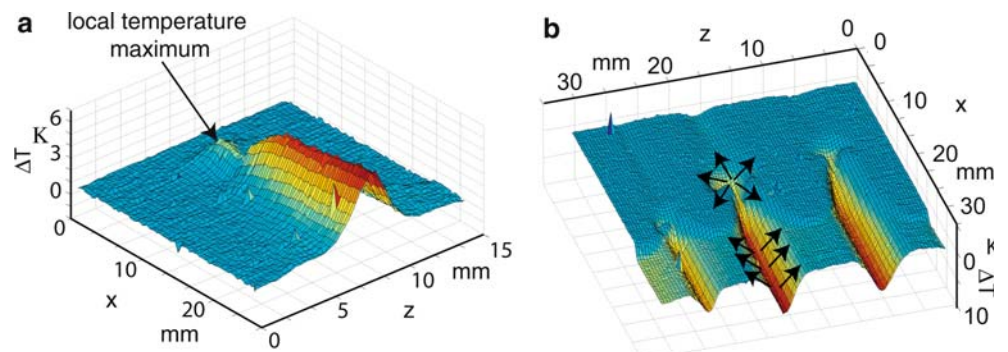


Figure 4a shows an enlargement of area A from Fig. 3c. The local temperature maximum, which forms the “head” of regular structures, is located in a field where two wave fronts intersect. Thereby the local temperature gradients are approximately equal. When the velocities of adjacent waves are different, the “head” is displaced in the direction of the slower wave.

We assume that the surface temperature is inversely proportional to the film thickness. Thus, it is possible to

make a qualitative statement about the hydrodynamics of the film when the temperature field is known. In Fig. 4b the surface temperature of area B from Fig. 3c is shown on an inverted scale. This illustrates the film thickness according to the supposition that the wave crests, which come along with a lower temperature, have higher thickness. In the enlargement the assumed flow lines are presented. This assumption still needs experimental coverage.

Fig. 4 Surface temperature field, DMS-T11, $Pr = 96$, $Re = 12.2$; **a** Local temperature maximum due to intersection of large waves, **b** surface temperature on an inverted scale and assumed direction of thermo-capillary flow



In Fig. 5 experimental data on the dimensionless distance between regular structures divided through the critical wavelengths of the Rayleigh–Taylor instability Λ_0 are presented. First of all, data were plotted against the Reynolds number. In Fig. 5a measured values are shown exemplary for a heat flux of $q_w = 0.4 \times 10^4 \text{ W m}^{-2}$ with excited waves. The values of the critical wavelength and the wavelength of maximum growth of the Rayleigh–Taylor instability are also shown in the same diagram at $\Lambda/\Lambda_0 = 1$ and $\Lambda/\Lambda_0 = \sqrt{3}$. Since the coefficients of the surface tension and the density almost remain constant for DMS-T05, DMS-T11 and DMS-T12 the values are very similar: $\Lambda_0 = 9.68, 9.70, 9.74 \text{ mm}$ and $\sqrt{3}\Lambda_0 = 16.76, 16.80, 16.86 \text{ mm}$, respectively. It is obvious from the diagram that for DMS-T05 and DMS-T11 the measured points are between these wavelengths and weakly depend on Reynolds number. This endorses the assumption that the nature of regular structure formation is connected with instability and the break up of 2D waves. Only for DMS-T12, Λ decreases with an increase in the Reynolds number. This is due to the fact that at low Reynolds numbers the liquid flow has a distinct 2D character and the high viscosity of the liquid impedes development of thermal-capillary phenomena. Standard deviations of regular structure sizes are presented selectively in the diagram. In the same diagram experimental data from [5] are presented for falling water films with natural waves. In [5] it was shown that $\Lambda \sim Re^n$, where the exponent n decreased from -0.028 to -0.310 with increasing heat flux. This tendency could not be validated with our experimental data. But it can be seen in Fig. 5a, that almost all points from [5] lie in the interval between $\Lambda/\Lambda_0 = 1$ and $\Lambda/\Lambda_0 = \sqrt{3}$.

Data for Λ averaged over all Reynolds numbers are shown in Fig. 5b against the heat flux. For example, all

data from Fig. 5a for silicone fluids could be found only in three points for a heat flux of $0.4 \times 10^4 \text{ W m}^{-2}$ in Fig. 5b. According to the diagram, there is no dependency of the size of regular structures on the heat flux. Almost all experimental points for DMS-T11 and DMS-T05 are between $\Lambda/\Lambda_0 = 1$ and $\Lambda/\Lambda_0 = \sqrt{3}$. Only in some range of the heat flux, data points corresponding to DMS-T12 are above $\Lambda/\Lambda_0 = \sqrt{3}$. The reason for this phenomenon has been described above. It can be seen from Fig. 5a that almost all data from [5] are in the interval between $\Lambda/\Lambda_0 = 1$ and $\Lambda/\Lambda_0 = \sqrt{3}$, too.

4 The model of thermal-capillary breakdown of laminar-wavy falling film

In analogy to [3] the force balance in the y – z plane within the residual layer is considered, Fig. 6. As it was already shown above, regular structures are formed in flow direction. Neglecting friction between the fluid and the surrounding gas phase as well as inertial effects in the fluid the balance between the forces of surface tension and the tangential stress becomes:

$$\mu \frac{\partial u_z}{\partial y} = \frac{d\sigma}{dz} = \frac{d\sigma}{dT} \frac{\partial T}{\partial z}. \quad (1)$$

Approximating Eq. 1 by a finite difference equation the characteristic “thermal-capillary” velocity can be expressed as

$$U_{TC} = \left| \frac{d\sigma}{dT} \right| \frac{\Delta T_z \delta_{res}}{\mu l_z}, \quad (2)$$

where ΔT_z is the characteristic temperature drop along l_z . Contrary to the model suggested in [3] l_z is not the characteristic length scale but equal to one half of the

Fig. 5 a Dimensionless dependency of the average length scales of regular structures on the Reynolds number by the falling film with excited waves. Data for water falling film with the natural waves [5]. **b** Dimensionless dependency of the average length scales of regular structures on heat flux. Data for water falling film for the natural waves [5]

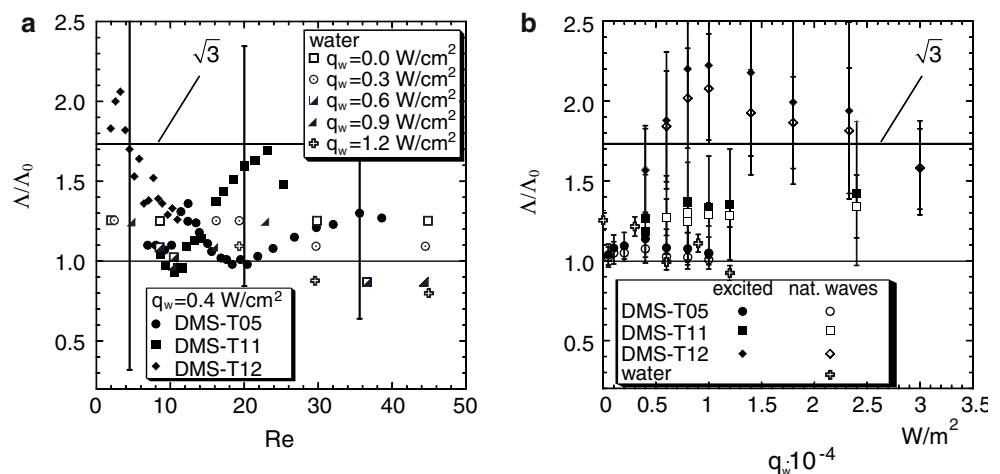
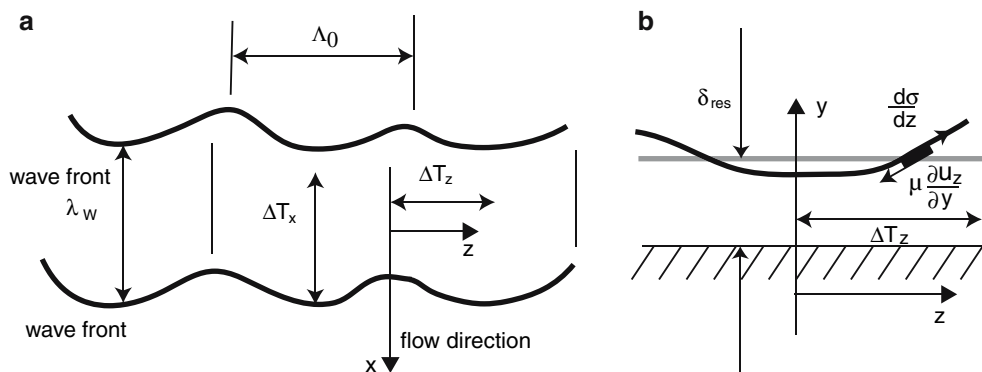


Fig. 6 **a** Schematic pattern of regular structures within the residual layer. **b** Thermal-capillary breakdown within the residual layer



distance between two structures as they can be determined in experiments:

$$l_z = \frac{\Lambda_0}{2}. \tag{3}$$

In analogy to [7] dry spots may appear in the film when the time required for thermal-capillary breakdown in the residual layer and the period between passing of two consecutive wave crests are of same order:

$$t_{TC} = t_w, \quad \text{there by } t_{TC} = \frac{l_z}{U_{TC}}, \quad t_w = \frac{1}{f_w} = \frac{\lambda_w}{c_w}, \tag{4}$$

and f_w is the dominating frequency of large wave propagation and λ_w is the length of large waves.

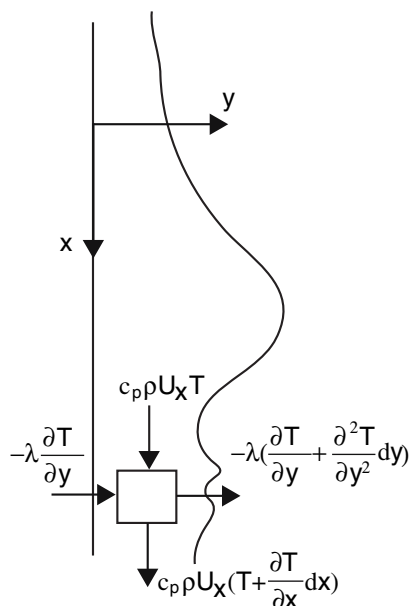


Fig. 7 Energy balance in the residual layer

Figure 7 shows the energy balance inside an infinitely small element in a film in the x - y plane. Neglecting the heat conduction in x direction and the convective heat transfer in y direction we obtain the equation:

$$\rho c_p \mu_x \frac{\partial T}{\partial x} = \lambda \frac{\partial^2 T}{\partial y^2} = -\frac{\partial q}{\partial y}. \tag{5}$$

Approximating this equation by a finite differential equation we can determine the typical temperature drop over $l_x \equiv 0.9\lambda_w$:

$$\Delta T_x = \frac{q_w}{\delta_{res}} \frac{0.9\lambda_w}{\rho c_p U_{res}}, \tag{6}$$

where q_w is the heat flux at the wall, U_{res} is the average liquid velocity in the residual layer, ρ is the liquid density and c_p is the specific heat. The remaining ten percent of l_x correspond to the length of the wave front. The material properties are taken at inflow temperature. From the thermographic pictures as presented in Fig. 3, the temperature difference in x and y direction can be evaluated. Thereby a proportionality can be determined.

$$\Delta T_z = k \cdot \Delta T_x. \tag{7}$$

As for current data the constant of proportionality is in the range between $1 < k < 5$. For further considerations a value of $k = 3$ was assumed.

$$\Delta T_z = 3\Delta T_x. \tag{8}$$

Now, substituting expressions (7) and (6) into (2), we obtain:

$$U_{TC} = \left| \frac{d\sigma}{dT} \right| \frac{1}{\mu} \frac{q_w}{l_z} \frac{0.9\lambda_w}{\rho c_p U_{res}} \frac{1}{3} \tag{9}$$

and (9) into (4):

$$\frac{1}{l_z} \left| \frac{d\sigma}{dT} \right| \frac{1}{\mu} \frac{q_w}{l_z} \frac{0.9 \lambda_w}{\rho c_p U_{res}} \frac{1}{3} = \frac{c_w}{\lambda_w} \tag{10}$$

c_w is the phase velocity of large waves.
Solving Eq. 10 for q_w :

$$q_w = \frac{1}{0.9} \frac{c_w}{\lambda_w^2} \frac{\rho c_p U_{res}}{\left| \frac{d\sigma}{dT} \right|} \frac{\mu l_z^2}{3} = \frac{1}{0.9} \frac{f_w^2}{c_w} \frac{\rho c_p U_{res}}{\left| \frac{d\sigma}{dT} \right|} \mu \frac{\Lambda_0^2}{4} \frac{1}{3}. \tag{11}$$

According to expression (11) the critical heat flux depends on the liquid properties, the frequency of large waves and the typical transverse size of regular structures. If the following dimensionless numbers are used:

$$Ma_q = \frac{q_w \left| \frac{d\sigma}{dT} \right| \left(\frac{v^2}{g} \right)^{\frac{2}{3}}}{\lambda \rho v^2}, Pr = \frac{v}{a} \text{ and } K_\Lambda = \left(\frac{f_w \Lambda_0}{(vg)^{\frac{1}{3}}} \right)^2. \tag{12}$$

Equation 12 can be presented in the form:

$$\frac{Ma_q}{Pr K_\Lambda} = \frac{1}{0.9} \frac{U_{res}}{c_w} \frac{11}{43} = \frac{1}{10.8} \frac{U_{res}}{c_w}. \tag{13}$$

Therefore, in Fig. 8 the experimental data for the dimensionless critical heat flux $\frac{Ma_q}{Pr K_\Lambda}$ are presented as a function of the Reynolds number. Only data which were obtained with activated loud speaker were used, allowing to keep the major frequency f_w at a constant value. As can be seen Eq. 13 depends on the relation between the mean velocity of the residual layer and the mean velocity of large waves. In the literature many different analytical and empirical equations can be found for these velocities as functions of the Reynolds number. For example in [4] a physical model for the falling film is presented. In this case the ratio between these velocities is constant:

$$\frac{U_{res}}{c_w} = 0.091. \tag{14}$$

Therefore the combination of dimensionless parameters from (13) is constant, too:

$$\frac{Ma_q}{Pr K_\Lambda} = 8.43 \times 10^{-3}. \tag{15}$$

Equation 15 is in the same order for the dimensionless critical heat flux as the experimental data, but the trend of the latter has a different inclination, see Fig. 8.

In [2] the same silicone oils were used as in the current experiments. Therefore a better comparability could be given for dependencies from [2] as for other correlations from literature. Since the thickness of the residual layer is relatively small we can use the Nusselt formula for laminar flow:

$$U_{res} = \frac{g \delta_{res}^2}{3\nu}. \tag{16}$$

In [2] an equation for the residual layer thickness can be found:

$$\delta_{res} = (1 + 0.219 Re^{0.6}) \left(\frac{v^2}{g} \right)^{\frac{1}{3}}. \tag{17}$$

Substituting (17) into (16):

$$U_{res} = \frac{1}{3} g^{\frac{1}{3}} v^{\frac{1}{3}} (1 + 0.219 Re^{0.6})^2 \tag{18}$$

and another equation from [2] giving the velocity of large waves against the Reynolds number:

$$c_w = 5.516 g^{\frac{1}{3}} v^{\frac{1}{3}} Re^{0.36}. \tag{19}$$

From Eq. 13 the following non-dimensional expression can be derived with substitutions (18) and (19):

$$\frac{Ma_q}{Pr K_\Lambda} = 5.6 \times 10^{-3} \frac{(1 + 0.219 Re^{0.6})^2}{Re^{0.36}}. \tag{20}$$

The comparison of dependence (20) with experimental data gives a good agreement in the order of magnitude but a difference in the inclination, see Fig. 8. For a Reynolds number range $Re < 3$ the dimensionless parameter $\frac{Ma_q}{Pr K_\Lambda}$ according to Eq. 20 even decreases, but the experimental data show another tendency.

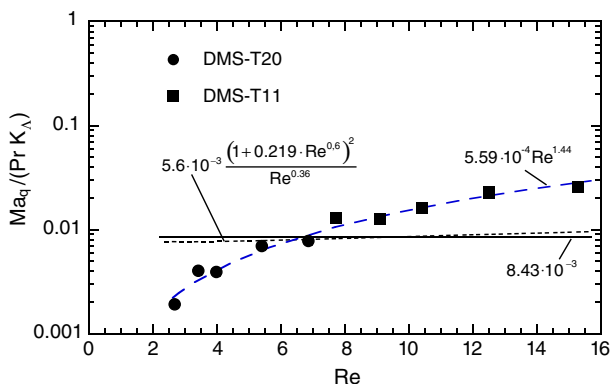


Fig. 8 The dependence of dimensionless parameter $\frac{Ma_q}{Pr K_\Lambda}$ versus the Reynolds-number. *Points* experimental data

This disagreement between experimental data and theory can be ascribed to the uncertainty of the proportionality factor in Eq. 7 as described above.

As can be seen from (20):

$$Ma_q = f(Re, Pr, K_\Lambda). \tag{21}$$

The approximation found from experimental data analysis is:

$$Ma_q = 5.59 \times 10^{-4} Re^{1.44} Pr K_\Lambda. \tag{22}$$

In order to verify and consolidate this theory the range of Reynolds numbers should be increased. The limitation of the variation of Reynolds numbers was described above. The next improvement will be an elongated heat section to allow for observation of further development of regular structures. For the experiments without activated loud speaker the wavelength has to be determined by measuring the oscillations of the film surface and using the major frequency for the parameter K_Λ .

A comparison of our experimental data with other dependencies from the literature can be found in the appendix.

5 Conclusions

For the first time regular structures have been revealed within the residual layer of laminar-wavy falling films using IR-thermography. Evolution of metastable quasi-regular structures on the surface of the film and the effect of structure existence on the pattern of large waves were studied experimentally. The visualisation showed that regular structures in the area of the residual layer appear at locations where two 3D waves intersect.

According to experimental data, the average values of transverse sizes of regular structures, Λ , are in the range between the critical wavelength $\Lambda_0 = 2\pi \sqrt{\frac{\sigma}{(\rho_l - \rho_g)g}}$ and the wavelength of maximum growth of the Rayleigh–Taylor instability.

A model of thermal-capillary breakdown of a liquid film and dry spot formation is suggested on the basis of a simplified force balance considering thermal-capillary forces in the residual layer. It is shown that the critical heat flux depends on half the distance between two hot structures, because the fluid within the residual layer is transferred from hot structures to the cold areas in between them. It also depends on the main frequency of large waves, the Prandtl number, the heat

conductivity, the liquid density and the change in surface tension $|\frac{d\sigma}{dT}|$. The model is also presented in a dimensionless form.

Results obtained are important for the investigation of the dependency between wave characteristics and local heat transfer, the conditions of “dry spot” enlargement and the development of crisis modes in intensely evaporating laminar-wavy falling films.

Acknowledgment This work was financially supported by the Deutsche Forschungsgemeinschaft (Project Re 463/31-1 and SFB 540) and the Russian Foundation of Basic Research (Project 03-02-04027-NNIO-a) in a collaboration project.

6 Appendix

In this part different approaches for the determination of the critical dimensionless heat flux are presented.

Experimental data for laminar-wavy and turbulent films were described in [8] by the following empirical dependencies:

$$Ma_q = 0.522 Re^{0.4} \left(1 + 0.12 \left(\frac{Re}{250} \right)^{4.5} \right)^{0.5} \text{ for } L \leq 1 \text{ m.} \tag{23}$$

For $100 < Re < 200$ in [8] the scattering of data was up to 50 %, for $Re < 100$ no experimental data has been recorded. It can be seen in Fig. 9 that this dependence suggests lower values than the current experimental data. The difference can be explained by the fact that in [8] the experimental data was obtained only for a water film flow with a relatively long heated section. In this case evaporation effects and thus a shift in the thermophysical properties could have appeared.

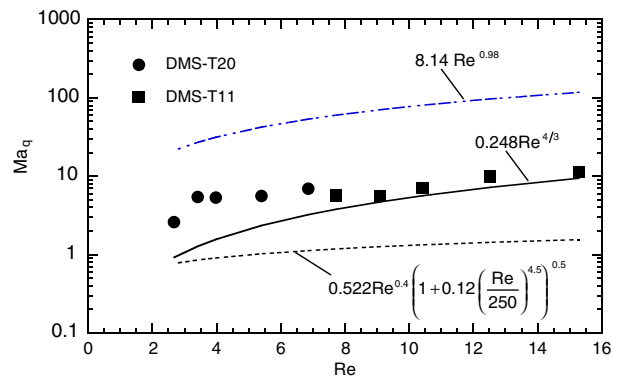


Fig. 9 The dependence of dimensionless parameter Ma_q versus the Reynolds-number. Points experimental data

In [10] the empirical dependence of the critical Marangoni number on the Reynolds number for a short heat section (6.5 mm length along the flow) for laminar waveless falling films was obtained:

$$Ma_q = 8.14Re^{0.98}. \quad (24)$$

In this case the length of the heated section is in the same order of magnitude as the thermal entry length [10]. Therefore this curve indicates higher values than our experimental data.

It was shown in [9] that for the 2D case the modified critical Marangoni number is constant:

$$Ma_c = \frac{q_w \left| \frac{d\sigma}{dT} \right|}{\lambda \rho U_s^2} = 0.23. \quad (25)$$

With the film surface velocity based on Nusselt's film theory $U_s = \frac{g}{2\nu} \delta_m^2$, expression (25) can be transformed into:

$$Ma_q = 0.248Re^{4/3}. \quad (26)$$

It can be seen, that only dependence (26) is in the same order of magnitude as our experimental data.

Other dimensionless parameters for generalisation of experimental data were used in [3] and [16]. In [3] the data for dimensionless breakdown heat flux is approximated in the form:

$$\frac{q_w \left| \frac{d\sigma}{dT} \right|}{\rho^{1/3} c_p \mu^{5/3} g^{2/3}} = 4.78 \times 10^5 Re^{1.43}. \quad (27)$$

With elementary transformations (27) can be transformed into:

$$\frac{Ma_q}{Pr} = 4.78 \times 10^5 Re^{1.43}. \quad (28)$$

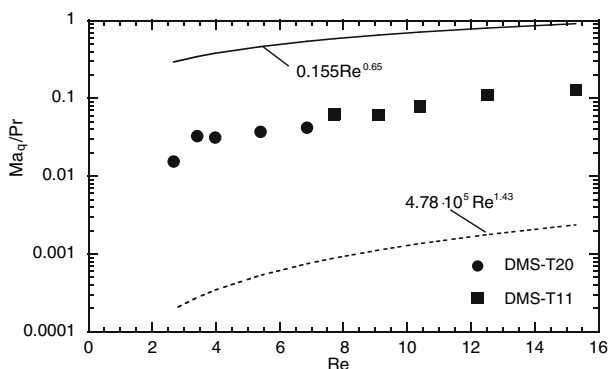


Fig. 10 The dependence of dimensionless parameter $\frac{Ma_q}{Pr}$ versus the Reynolds-number. Points experimental data

Figure 10 shows that (28) again leads to lower values than our experimental data. Here, as in case of Eq. 23, evaporation effects could have appeared, because this dependence was obtained for water and for a 30% glycerol–water solution at a 2.5 m long test section for $Re > 959$.

A generalisation for water and aqueous solution of alcohol is presented in [16]:

$$\frac{Ma_q}{Pr} = 0.155Re^{0.65}. \quad (29)$$

This correlation leads to results which exceed current data by more than one order of magnitude. It can be partially explained by the fact that dependence (29) was obtained for stable dry spots, whereas the new data was recorded for the formation of local instable dry spots.

References

1. Al-Sibai F, Leefken A, Lel VV, Renz U (2003) Measurement of transport phenomena in thin wavy film. Fortschritt-Berichte VDI 817 Verfahrenstechnik Reihe 3:1–15
2. Al-Sibai F (2004) Experimentelle Untersuchung der Strömungscharakteristik und der Wärmeübertragung bei welligen Rieselfilmen. Thesis of Dr.-Ing. Degree, Lehrstuhl für Wärme- und Stoffübertragung, RWTH Aachen
3. Bohn MS, Davis SH (1993) Thermo-capillary breakdown of falling liquid film at high Reynolds numbers. Int J Heat Mass Transf 7:1875–1881
4. Brauner N, Maron DM (1983) Modeling of wavy flow in inclined thin films. Chem Eng Sci 38(5):775–788
5. Chinnov EA, Kabov OA (2003) Jet formation in gravitational flow of a heated wavy liquid film. J Appl Mech Tech Phys 44(5):708–715
6. El-Genk MS, Saber HH (2002) An investigation of the breakup of an evaporating liquid film, falling down a vertical, uniformly heated wall. J Heat Transf Trans ASME 124(1):39–50
7. Ganchev BG (1984) Hydrodynamic and heat transfer processes at downflows of film and two-phase gas–liquid flows (in Russian). Thesis of Doctor's Degree in Phys-Math. Sci., Moscow
8. Gimbutis G (1988) Heat transfer at gravitation flow of a liquid film, Mokslas, Vilnius (in Russian)
9. Ito A, Masunaga N, Baba K (1995) Marangoni effects on wave structure and liquid film breakdown along a heated vertical tube. In: Serizawa A, Fukano T, Bataille J (eds) Advances in multiphase flow. Elsevier, Amsterdam, pp 255–265
10. Kabov OA (2000) Breakdown of a liquid film flowing over the surface with a local heat source. Thermophys Aeromech 7(4):513–520
11. Kabov OA, Chinnov EA (1998) Hydrodynamics and heat transfer in evaporating thin liquid layer flowing on surface with local heat source. In: Proceedings of 11th international heat transfer conference, vol 2, August 23–28, Kyondju, Korea, pp 273–278
12. Nusselt W (1916) Die Oberflächenkondensation des Wasserdampfes. Z VDI 60:541–546

13. Pavlenko AN, Lel VV (1997) Heat transfer and crisis phenomena in falling films of cryogenic liquid. *Russ J Eng Thermophys* 3–4(7):177–210
14. Pavlenko AN, Lel VV, Serov AF, Nazarov AD, Matsekh AM (2002) Wave amplitude growth and heat transfer in falling intensively evaporating liquid film. *J Eng Thermophys* 11(1):7–43
15. Wang BX, Zhang JT, Peng XF (2000) Experimental study on the dryout heat flux of falling film. *Int J Heat Mass Transf* 43:1897–1903
16. Zaitsev DV, Kabov OA, Cheverda VV, Bufetov NS (2004) The effect of wave formation and wetting angle on the thermocapillary breakdown of a falling liquid film. *High Temperature* 42(3):450–456